IMPROVED HEAT SWITCH FOR GAS SORPTION COMPRESSOR

Chung K. Chan

Jet Propulsion Laboratory
California Institute of Technology
4800 Oak Grove Drive
Pasadena, California 91109

Thermal conductivities of the charcoal bed and the copper matrix for the gas adsorption compressor were measured by the concentric-cylinder method. The presence of the copper matrix in the charcoal bed enhanced the bed conductance by at least an order of magnitude. Thermal capacities of the adsorbent cell as well as the heat leaks of two compressor designs were measured by the transient method. The new gas adsorption compressor had a heat switch that could transfer eight times more heat than the previous one. Because of this, the cycle time for the new prototype compressor was also improved by a factor of eight to within the minute range.

Key words: Charcoal bed; copper foam; gas adsorption; gas heat switch; heat capacitance; refrigerator; switch ratio; thermal conductance.

1. Introduction

In the gas sorption refrigeration cycle, whether it is the gas adsorption system [1,2] or the gas absorption system [3,4], the sorption (adsorbent or absorbent) bed must be cycled between the temperature of the heat source and the temperature of the reservoir to which heat is being rejected. Thus, making and breaking thermal contacts of the sorption bed with the reservoirs are essential operations. A similar situation exists for the salt bed of the magnetic refrigerator. Heat switches based upon different physical mechanisms have been developed. Mechanically actuated heat switches [5] have been proved unreliable at cryogenic temperatures, and require large contact force. Magnetoresistive heat switches [6] are, except at very low temperatures, of very low efficiency and require a magnetic field. Gaseous thermal switches [7,8] which are probably the oldest idea, depend on the switching action resulting from the presence or absence of the gas. Efficient gaseous switches require a small gas gap but large heat transfer areas which are sometimes hard to achieve. Since the primary goal of the sorption refrigerators is one of lifetime and reliability, it was decided to use a reliable gas heat switch for the adsorption compressor [9].

Since the switching function in the gaseous heat switch is accomplished by the presence and absence of the gas between two surfaces, gas supply and a suction pump are required. These functions are provided by an adsorption pump connected to the switch. In our earlier gas adsorption compressor (GAR-I) [9] the heat switch in each compressor unit was controlled by a miniature pump. In our current modular design (GAR-II), each compressor unit has one heat switch but four heat switches are controlled by one pump [10].

One majc · difficulty in the gas adsorption or desorption process is to transport heat into and out of the porous media rapidly. In the GAR-I design, because of this limitation, the cycle time of the gas sorption refrigerator was in the range of six to fifteen minutes. This time was too long for a practical refrigerator. As an ongoing development effort of nonmechanical (gas adsorption or absorption) refrigerators for spaceborne instruments, research has been performed to study the heat transfer characteristics of the porous charcoal medium, the porous medium enhanced by a metal matrix, and the gas heat switch. This paper presents the results of these research efforts that lead to the construct :n of the rapidly cycled compressor [10].

2. Thermal conductance and gas adsorption compressor designs

The thermal properties of charcoal beds with heat transfer enhancement element are essential data for compressor design and performance analyses. The thermal conductivity of a bed of charc · was measured in the temperature range between 20C and 475C, using a conventional steady-state method, the so-called concentric-cylinder method, with the inner cylinder being a heater. The charcoal particles (200 μm - 400 μm in size) were filled into the space between the heater and an outer stainless steel cylinder. The heat flow was radial as the length of the cylinder (L) was large (5.1 cm) compared to the distance between the cylindrical shells (0.85 cm). The temperature gradient due to the radial heat flow was measured by two thermocouples located at radii r_i and r_o, close to the mid-point of the cylinder. The thermal conductance k of the bed was calculated from the following relation:

$$k = \frac{\dot{Q}\ln(r_o/r_i)}{2\pi L(T_i - T_o)} \qquad (1)$$

where k = thermal conductance (W/cmK)
$\dot{Q}$ = power of the central heater (Watt)
T_i, T_o = temperatures measured at radii r_i, r_o, respectively

With r_i = 0.31 cm and r_o = 1.17 cm, the results for the thermal conductivities k of the charcoal bed are listed in Table 1. Thermal conductivities between 1.17×10^{-3} W/cmK and 1.26×10^{-3} W/cmK are found. These values are in the same order of magnitude as those of the zeolite bed reported in the literature [11].

Table 1. Thermal conductance of charcoal bed

T_i(C)	T_o(C)	$\dot{Q}$(W)	$k\left(\frac{W}{cmK}\right)$
229	59	4.45	1.17×10^{-3}
295	78	6.24	1.17×10^{-3}
365	90	8.19	1.22×10^{-3}
420	104	9.49	1.23×10^{-3}
475	116	11.12	1.26×10^{-3}

The thermal conductivity of a copper foam (3% by volume) was determined by the similar method and the value was listed in Table 2. It was observed that the copper foam had thermal conductivity an order of magnitude better than the charcoal bed. Hence, when the charcoal was packed into the copper foam matrix, the thermal conductance of the bed would be increased by an order of magnitude. Because of this heat enhancement, in our earlier adsorption compressor (GAR-I), as shown in Fig. 1, 7.38 gm of charcoal which was confined within a stainless steel cylinder of volume 14.35 cm^3, was packed into the open foam copper matrix. The temperature of the adsorbent cell was controlled by a 40 W heater and a gas heat switch gap to a 77 K heat sink. The presence and absence of the gas in the gap are controlled by a miniature adsorption pump containing a small amount of charcoal. A schematic of the adsorbent bed, the heat switch and the miniature pump is shown in Fig. 1.

Table 2. Thermal conductance of copper foam

T_i(C)	T_o(C)	$\dot{Q}$(W)	$k\left(\frac{W}{cmK}\right)$
46	44	2.15	0.040
76	69	4.66	0.026
144	130	11.28	0.033
195	170	16.7	0.027
274	227	28.1	0.024

The heat path from the adsorbent bed to the 77 K heat sink passes through the porous bed and the stainless steel wall and is interrupted by the 0.18 mm annular gap between the inner stainless steel cylinder and the outer brass cylinder before it reaches th 77 K heat sink. The gap may be vacuum or filled with hydrogen gas through the stainless-steel capillary tube C, depending on the temperature of the miniature adsorption pump. The pump is maintained in weak thermal contact with the heat sink through an appropriately sized wire. A heater and a silicon diode were attached to the pump chamber.

The pump chamber was leak tested, vacuum outgassed and backfilled with hydrogen at 77 K and 200 torr. At that temperature all the gas was adsorbed onto the charcoal and there was no gas in the heat switch gap, i.e., the heat switch was off. When the pump was heated to about 110 K, the gas was released and the pressure built up. Hydrogen began to flow from the pump to the gas gap, i.e., the switch was on. Hydrogen was chosen because of its relative high thermal conductivity. The test results are presented in the next session.

The new refrigerator design (GAR-II) of 250 mW at 20 K consists of banks of individual compressor modules. A schematic of a modular design is shown in Fig. 2. This design involves four banks (A, B, C and D) containing sixteen compressor modules in total. Each compressor module is a double walled cylindrical unit as shown in Fig. 3. The charcoal, confined within the stainless steel inner pressure vessel, is packed into an open copper matrix foam. The gap between the inner and the outer cylinders is the gas heat switch. The heat switches of four compressors are controlled by one miniature adsorption pump of charcoal which when heated supplies gas to the switch, turning it on and when cooled, removing gas from the switch, turning it off. Each bank has one such miniature adsorption pump, so all the compressors in each bank are cooled at the same time.

3. Transient experimental measurements and results

Transient thermal tests were performed for the GAR-I compressor (Fig. 1) and the GAR-II compressor module (Fig. 3) to determine the heat capacity of the adsorbent bed, the heat leak, and the switching capacity of the heat switch.

In the tests involving the heat capacity, both the adsorbent cell and the heat switch pump were evacuated. The adsorbent cell was then heated, and the transient temperature was recorded. As the first iteration, the heat leak was ignored and the heat capacity of the adsorbent cell $(mc_p)_{cell}$ which included the charcoal, the stainless steel vessel and the copper foam was determined by

$$(mc_p)_{cell} = \frac{\dot{Q}}{\left(\frac{dT_a}{dt}\right)} \qquad (2)$$

where $\dot{Q}$ = heat input

$\frac{dT_a}{dt}$ = transient temperature gradient of the cell

The heat leak K_L from the cell was determined by recording the temperature during the cool down of the cell:

$$K_L = \frac{(mc_p)_{cell}}{t_f - t_i} \ln\left(\frac{T_i - T_s}{T_f - T_s}\right) \tag{3}$$

where T_i, T_f are temperatures at times t_i and t_f

T_s is the heat sink temperature

With the knowledge of the heat leak, as a second iteration the heat capacity was recalculated by

$$(mc_p)_{cell} = \frac{Q - K_L(T_a - T_s)}{\left(\frac{dT_a}{dt}\right)} \tag{4}$$

where T_a is the adsorbent cell temperature.

The heat capacities of the GAR-I adsorbent cell calculated by equations (2) and (4) are shown in Fig. 4. A theoretical curve based on the properties of carbon, stainless steel and copper is also shown in the same figure for comparison. It was observed that the experimental data were about 30% higher than the theoretical prediction. Fig. 5 shows the response of the switch to the heating of the charcoal pump. Within 50 seconds the switch is conducting. The value of the conductance K can be determined from the temperature transient by an energy balance of the adsorbent cell:

$$[(mC_p)_a + (mC_p)_{s.s.} + (mC_p)_c] \frac{dT_a}{dt} = -K(T_a - T_s) \tag{5}$$

where m is the mass

C_p is the heat capacity

the subscripts a, s.s. and c represent the adsorbent, the stainless steel vessel and the copper foam, respectively

$\frac{dT_a}{dt}$ is the gradient of the temperature transient

T_s is the heat sink temperature

The thermal conductance K was plotted as a function of the mean temperature, i.e., $(T_a + T_s)/2$ in Fig. 6. The theoretical K was calculated by knowing the heat switch area A, the gap size δ and the thermal conductivity k_g of the gas as

$$K = \frac{k_g A}{\delta} \tag{6}$$

Thus, with hydrogen as the working gas, the switch of GAR-I has a conductance of 0.8W/K when the switch is on and a conductance of 0.14W/K when the switch was off, giving a switch ratio of 5.7.

Similar tests were performed for the GAR-II compressor, and the results are shown in Figs. 7, 8 and 9. The thermal conductance of this new heat switch design was found to be 8 times better than the previous design. The switch of GAR-II has a conductance of 5W/K when the switch was on and a conductance of 0.37W/K when the switch was off, giving a switch ratio of 14.

4. Conclusions

The thermal properties of the adsorbent bed and the heat switch were determined by steady state and transient experiments. Results of these heat transfer studies led to the design and the construction of a new gas sorption compressor which had a heat switch that could transfer 5 W/K of heat from a 6 cm (H) x 2.54 cm (D) cylindrical modular compressor. Because of this, the cycle time for the new prototype compressor was about one minute. Since the system weight is almost inversely proportional to the cycle time, this improvement will no doubt reduce the refrigerator weight in spaceborne missions.

The research described in this paper was carried out by the Jet Propulsion Laboratory, California Institute of Technology, through contract with the National Aeronautics and Space Administration.

5. References

[1] Chan, C. K., Cryogenic refrigeration using a low temperature heat source, Cryogenics 21, 391-399 (1981).

[2] Chan, C. K., Tward, E. and Elleman, D. D., Miniature J-T refrigerators using adsorption compressor, Advances in Cryogenic Eng. 27, 735-743 (1981).

[3] Lehrfeld, D. and Boser, O., Absorption-desorption compressor for spaceborne/airborne cryogenic refrigerators, AFFDL-TR-74-221, AF Flight Dynamics Laboratory, Wright-Patterson AFB.

[4] Jones, J., $LaNi_5$ hydride cryogenic refrigerator test hardware results, Refrigerator for Cryogenic Sensors, NASA Conference Publication 2287, 357-373 (1982).

[5] Siegwarth, J. D., A high conductance helium temperature heat switch, Cryogenics 16, No. 2, 73-76 (1976).

[6] Radebaugh, R., Electrical and thermal magnetoconductivities of single-crystal beryllium at low temperatures and its use as a heat switch, J. of Low Temperature Physics 27, 91-105 (1977).

[7] Torre, J. P. and Chanin, G., Heat switch for liquid helium temperatures, Rev. Sci. Instrum. 55, 213-215 (1984).

[8] Tward, E., Gas heat switches, NBS Special Publication 607, Boulder, CO, 178-187 (1981).

[9] Chan, C. K., Tward, E., and Elleman, D. D., Kinetics of gas adsorption compressor, Advances in Cryogenic Engineering 29, 533-542, (1983).

[10] Chan, C. K., Performance of rapid cycled gas adsorption compressor, paper presented at the 10th International Cryogenic Conference, Helsinki, Finland, July 31-August 3, 1984.

[11] Volkl, J., Heat conduction in zeolite beds, Heat Transfer 1982, 2, C018, 105-108.

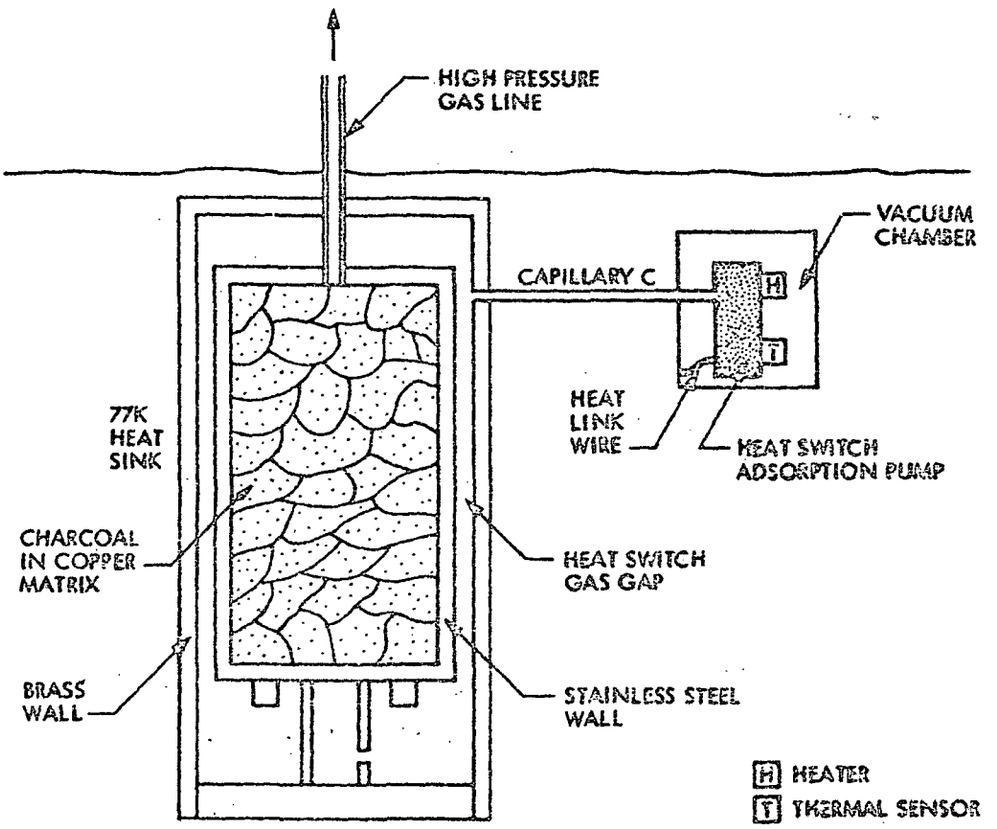

FIG. 1. GAR - I COMPRESSOR

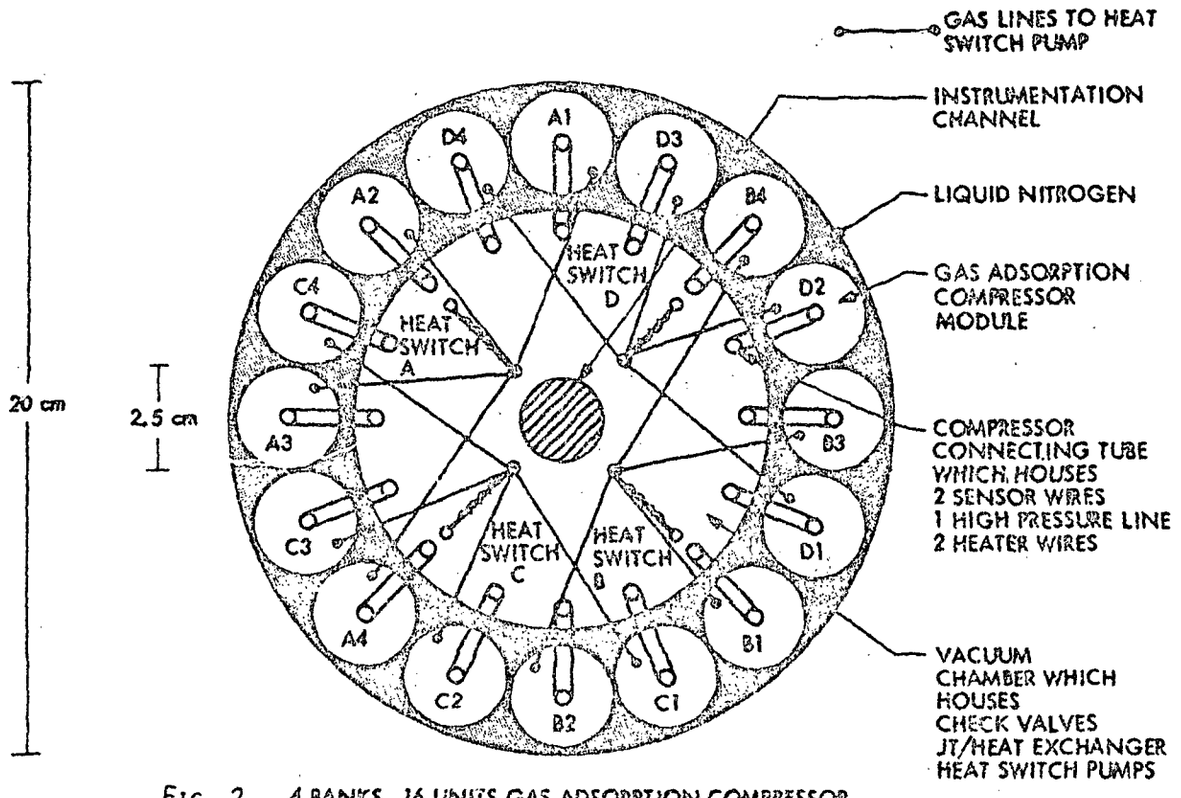

FIG. 2. 4 BANKS, 16 UNITS GAS ADSORPTION COMPRESSOR MODULAR DESIGN

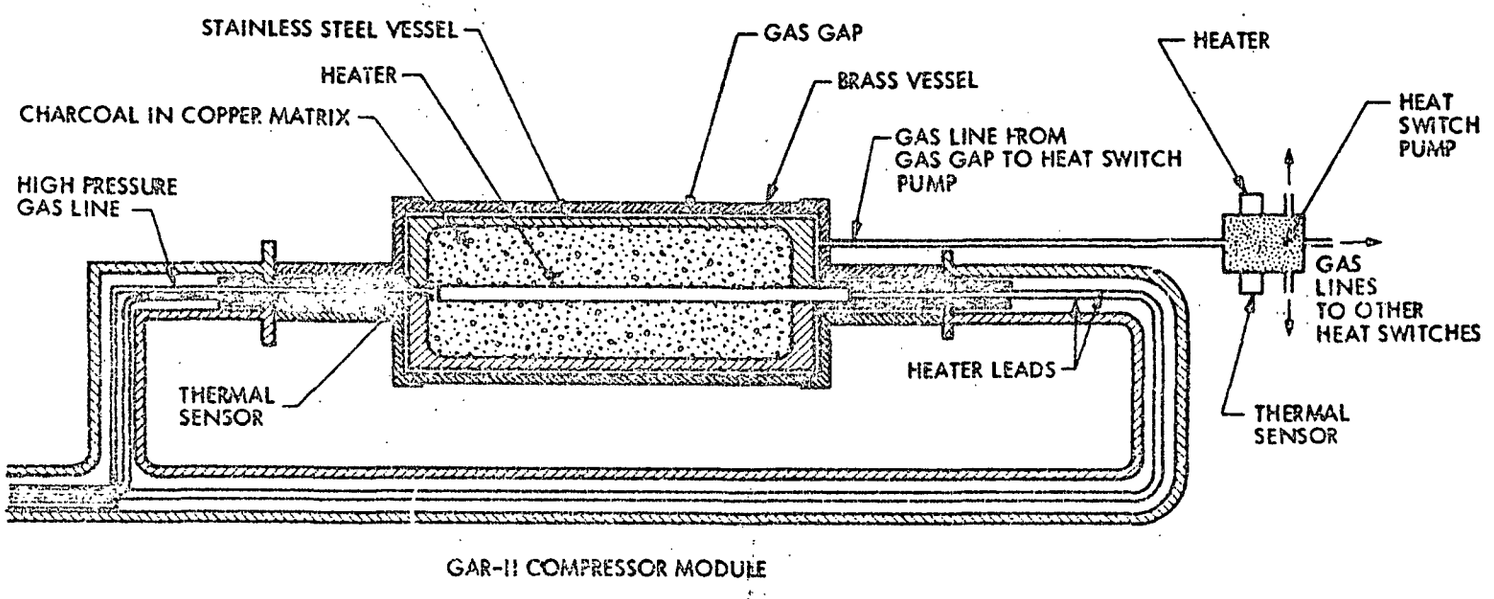

FIG. 3. GAR - II COMPRESSOR MODULE

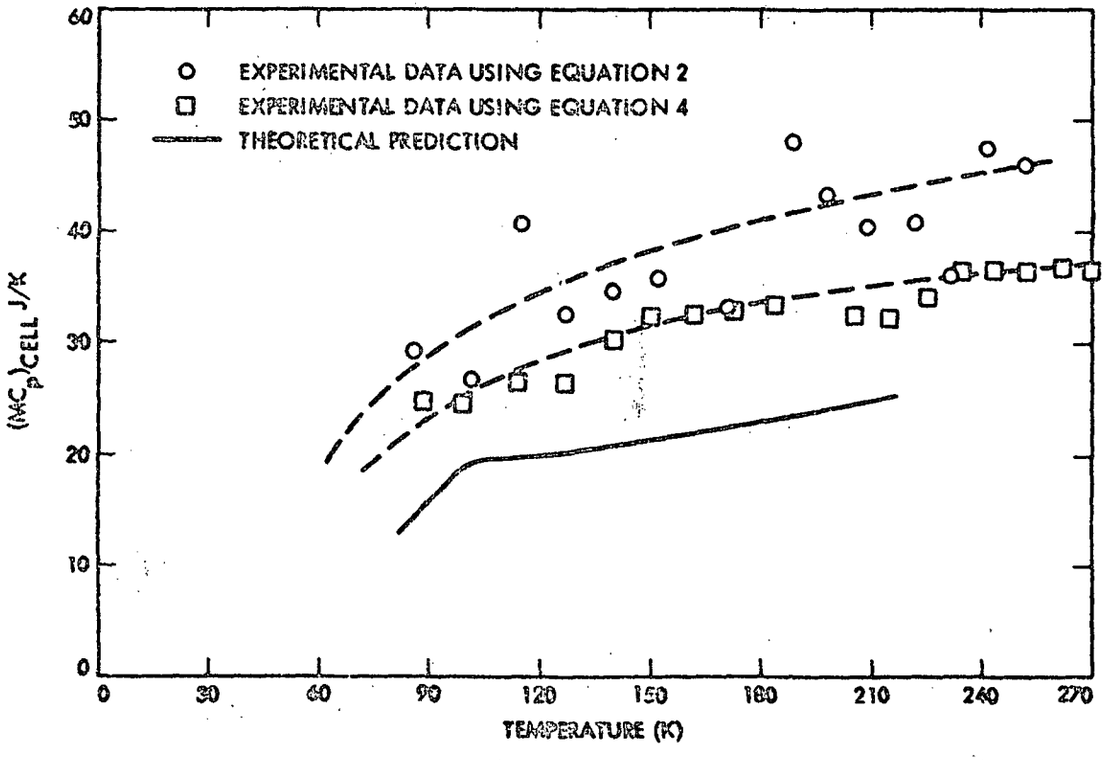

FIG. 4. HEAT CAPACITANCE OF THE GAR-I ADSORPTION CELL

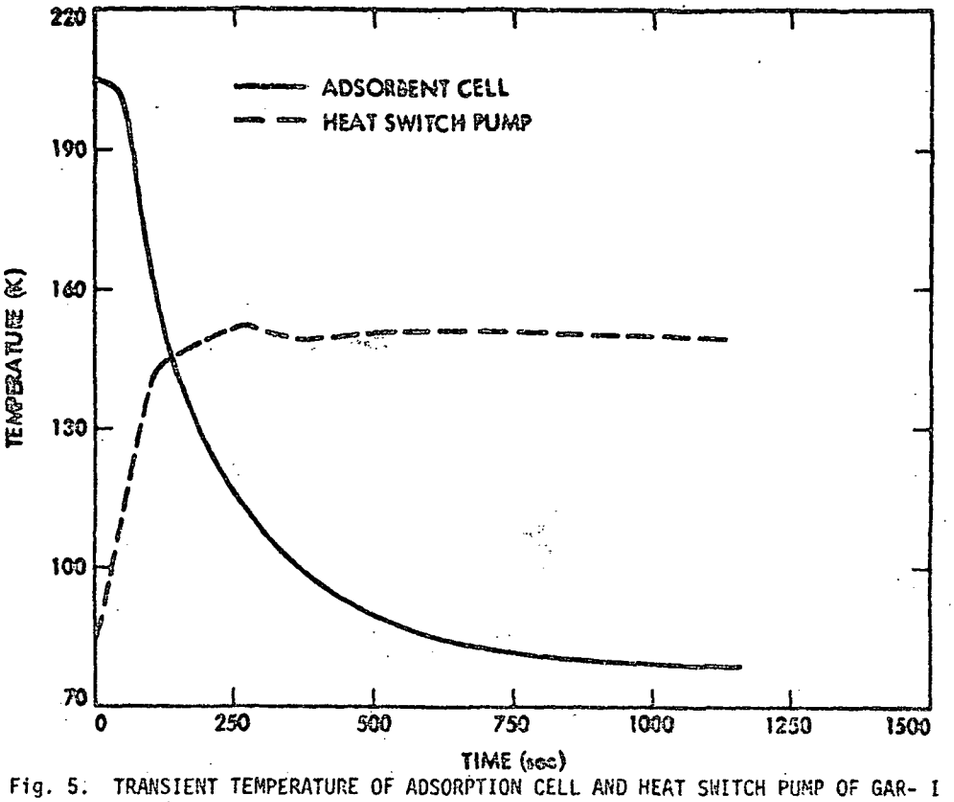

Fig. 5. TRANSIENT TEMPERATURE OF ADSORPTION CELL AND HEAT SWITCH PUMP OF GAR- I

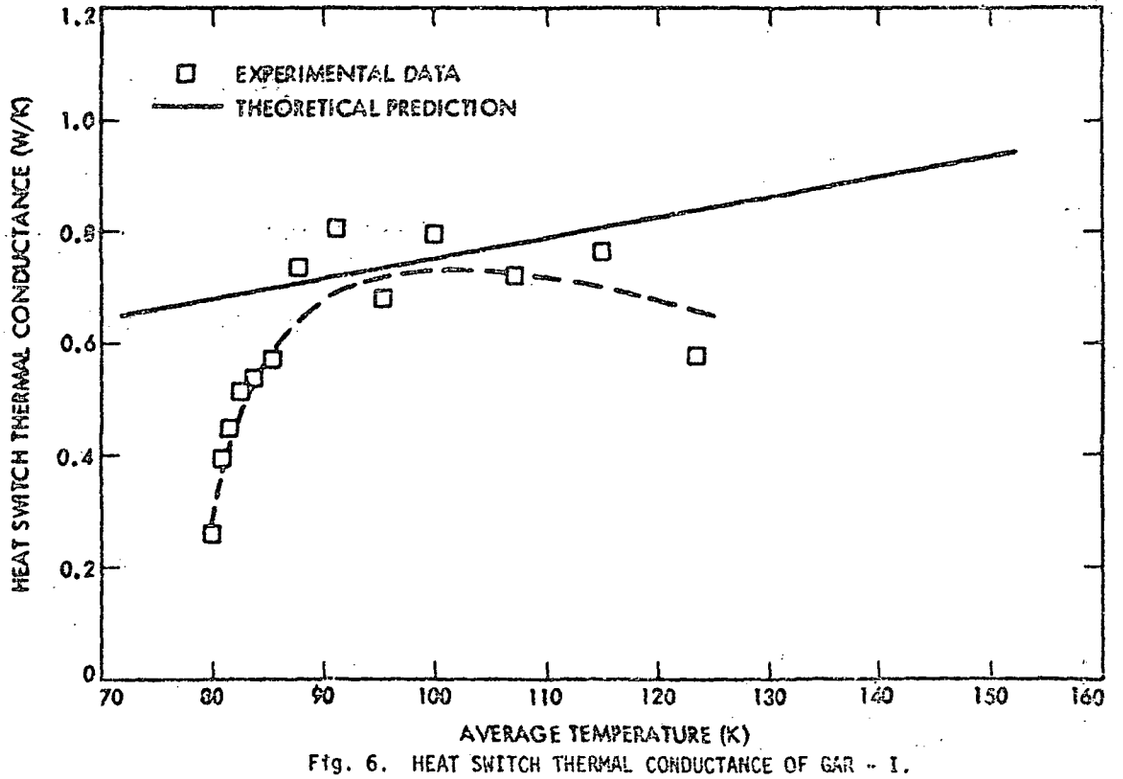

Fig. 6. HEAT SWITCH THERMAL CONDUCTANCE OF GAR - I.

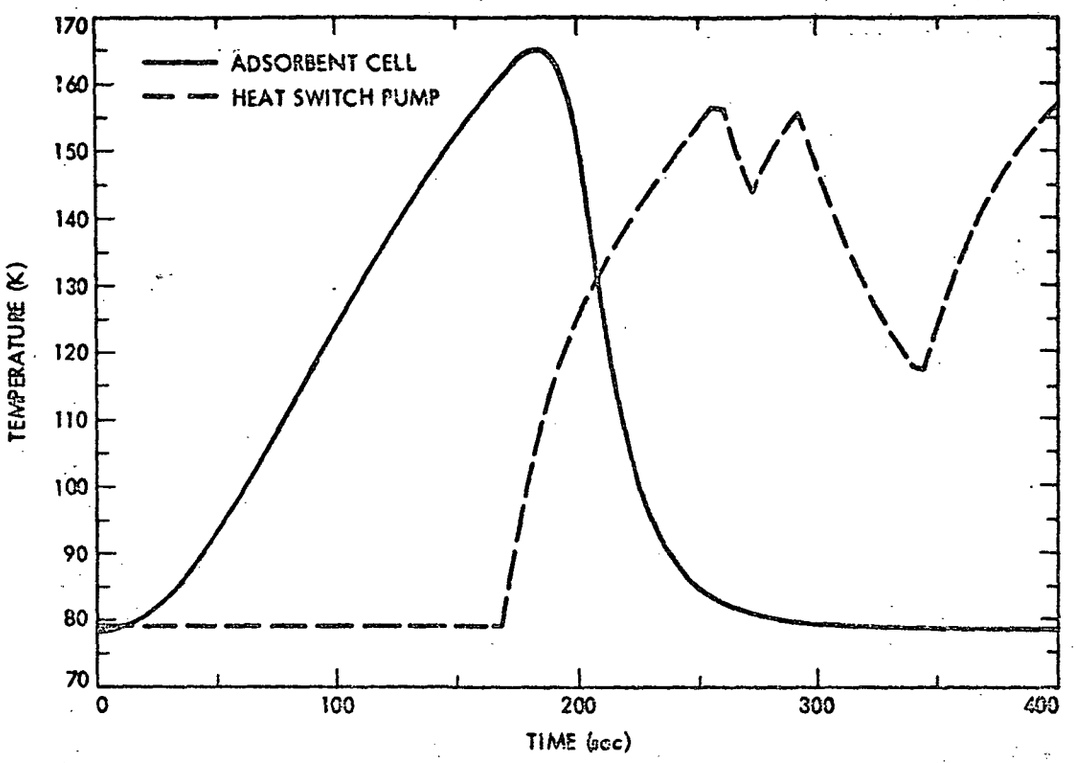

Fig. 7. TRANSIENT TEMPERATURES OF ADSORBENT CELL AND HEAT SWITCH PUMP OF GAR - II.

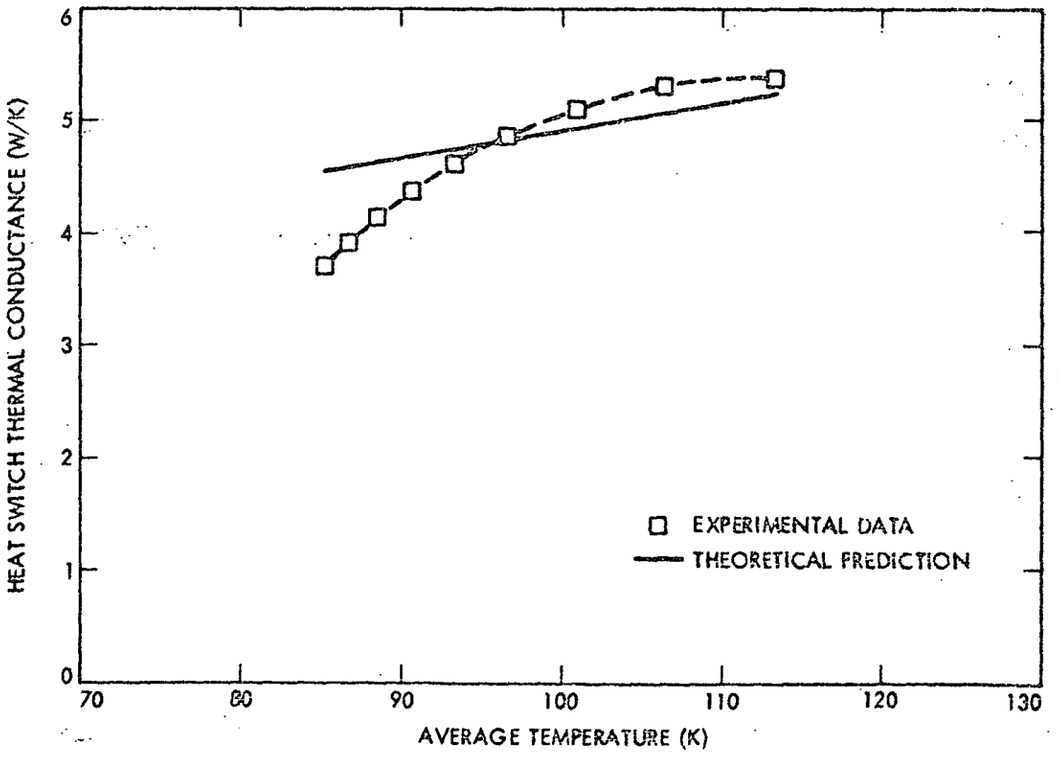

FIG. 8. HEAT SWITCH CONDUCTANCE OF GAR - II.